Explicit Constructions in the Modified Moving Sofa Problem

Jordan Fields

May 2020

1 Abstract

Posed by Leo Moser in a 1967 SIAM article, the moving sofa problem remains unsolved. Significant progress was made in Joseph Gerver's 1992 work *On Moving a Sofa Around a Corner* and then later in Dan Romik's 2016 work *Differential Equations and Exact Solutions in the Moving Sofa Problem*. While neither of these researchers were able to solve the moving sofa problem, they were able to establish some necessary conditions that the solution must meet. In this paper, we generalize the results of Romik (and implicitly Gerver) to a larger class of geometric optimization problems and conjecture their solutions.

2 A Brief History

In 1967, Leo Moser asked the question

> "what is the shape of largest area in the plane that can be moved around a right-angled corner in a two-dimensional hallway of width 1?"

Despite the problem's simple statement, it remains unsolved. Notable points of progress in the problem's history begin in 1968 with the work of John Hammersley who conjectured that his construction (*Figure 2*) of area $2/\pi + \pi/2 = 2.2074...$ was optimal. Hammersley's shape came as a consequence of two simple observations. The first observation was that a unit square was the shape of maximum size that could traverse the hallway by translation with no rotation. It simply travels up the vertical arm of the hallway until it cannot move any further, and then translates to the left along the horizontal arm. Similarly, a half circle of area $\pi/2$ is the shape of maximum size that can move through the hallway by rotation *and* translation. The movement of the semicircle can be described as first translating up the vertical arm, rotating by an angle of $\pi/2$, and then translating to the left through the horizontal arm. The movement of these two shapes is shown below in *Figure 1*. Hammersley assumed that the solution to the moving sofa problem would move through the hallway by a combination of both rotation and translation. He then reasoned that this shape would likely be some combination of the maximum shapes for the rotation only case and the translation only case. Hammersley divided the semicircle of area π into two equal halves and glued them

the sides of the unit square. Then, he carved a semicircle of area $2/\pi$ out of the square to allow it to rotate around the corner. This Frankenstein creation is known as Hammersley's sofa and was conjectured to be the solution to the Moving Sofa problem for over 20 years.

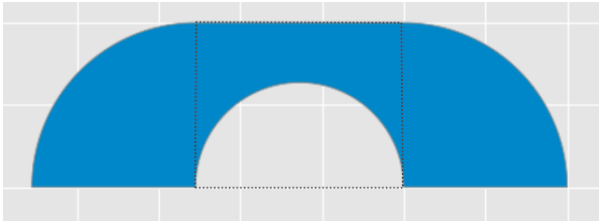

Figure 1: Hammersley's Sofa

In 1992 came the work of Joseph Gerver who found a valid construction (*Figure 2*) of area 2.2195... which was a modest improvement over Hammersley's construction.

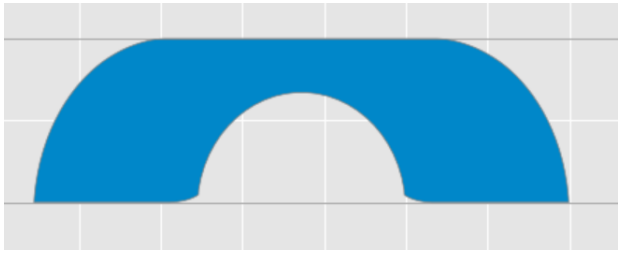

Figure 2: Gerver's Sofa

However, Gerver's results were interesting for reasons other than an increase in area over Hammersley's sofa. Whereas Hammersley's construction was a bit of a haphazard guess, Gerver's work formed the beginnings of what has become the conceptual framework for understanding the Moving Sofa Problem. Gerver defined a method for producing a sequence of finite polygonal intersections and proved that the sequence when taken to its limit converges to a solution to the moving sofa problem. Each of these finite polygon intersections satisfies a property which Gerver proved a solution to the Moving Sofa problem must also satisfy known as Gerver's *balanced condition*.

This condition states that a finite polygon intersection (in the context of the moving sofa problem) is *balanced* if each parallel edge one unit apart is of equal length. Gerver's proof that a solution must satisfy this condition is quite long at over five pages. In short, this condition is the discrete equivalent of saying that a solution to the moving sofa problem must not increase in area when small perturbations are made to its boundary. Otherwise, a small perturbation could be made to increase the area of the planar object contradicting the assumption that the previous shape was a solution at all. Using this fact, Gerver derived a new shape with a slightly larger area than that of Hammersley's sofa. By leveraging his balanced condition, Gerver was able to show that his shape is a local maximum and it remains the largest shape discovered to date. However, his conjecture of global optimality remains unproven. In fact, it is not even known whether the solution to the Moving Sofa Problem is unique. Note the use of the indefinite article *a* throughout the description of Gerver's

results. He was well aware of the fact that there could be an multitude of constructions which solve the moving sofa problem.

3 Romik's Framework and Preliminary Definitions

Romik began by establishing a *sofa-centric framework* as a way to understand the shape of the sofa as a function of the translation and rotation of the hallway around it. He defined the $L-$shaped hallway as

$$\begin{aligned} L_{horiz} &= \{(x,y) \in \mathbb{R}^2 : x \leq 1, 0 \leq y \leq 1\} \\ L_{vert} &= \{(x,y) \in \mathbb{R}^2 : y \leq 0, \leq x \leq 1\} \\ L &= L_{horiz} \cup L_{vert} \end{aligned}$$

Let $x : [0, \pi/2] \to \mathbb{R}^2$ be a continuous path satisfying $x(0) = (0,0)^T$. This defines the *rotation path*, the function which describes the movement of the the inner corner of the hallway as it is pushed around the plane. We also need to describe the rotation of the hallway as it moves around the sofa. Romik assumes (fairly) that the solution to the moving sofa problem will rotate around the hallway monotonically, so he describes the rotation of the hallway with R_t the rotation matrix given by

$$R_t = \begin{pmatrix} \cos t & -\sin t \\ \sin t & \cos t \end{pmatrix}$$

Let S be a planar shape which can move around the hallway (or equivalently have the hallway moved around it). Let $\lambda : \mathbb{R}^2 \to \mathbb{R}$ be a function which takes connected shapes in the plane and computes their area. Call S' the maximum sofa if $\lambda(S') > \lambda(S)$ for all connected $S \in \mathbb{R}^2$ satisfying

$$S \subseteq L_{horiz} \cap \bigcap_{0 \leq t \leq \pi/2} \Big(x(t) + R_t(L)\Big) \cap \Big(x(\pi/2) + R_{\pi/2}(L_{vert})\Big)$$

This is due to the fact that, in the sofa-centric framework, the sofa S must fit within (be a subset of) the hallway at each of its positions in the plane. Naturally this leads to the sofa S also being a subset of the infinite intersection. In fact, for a given rotation path $\mathbf{x}$, the maximum sofa which can navigate the hallway with a motion described by that path is given by the equality statement

$$S_{\mathbf{x}} = L_{horiz} \cap \bigcap_{0 \leq t \leq \pi/2} \Big(x(t) + R_t(L)\Big) \cap \Big(x(\pi/2) + R_{\pi/2}(L_{vert})\Big)$$

where $S_{\mathbf{x}}$ is the planar shape associated with the rotation path $\mathbf{x}$ in this way. Since the object we are looking for is the largest shape which fits in the hallway at each point of its rotation and translation in the plane, any shape which is not the entire intersection is smaller than the maximum. Romik writes that the natural question which remains is how to describe the map of $\mathbf{x} \to S_{\mathbf{x}}$. Romik answered this question by defining *contact points*, which are the points of tangency between the four walls of the hallway and the boundary of the shape $S_{\mathbf{x}}$.

He labels the contact points $\mathbf{A}, \mathbf{B}, \mathbf{C}$, and $\mathbf{D}$ where $\mathbf{A}$ and $\mathbf{C}$ correspond to the outer walls and $\mathbf{B}$ and $\mathbf{D}$ correspond to the inner walls. These points, as they move as functions of t, trace out *contact paths* denoted by $\mathbf{A}(t)$, $\mathbf{B}(t)$, $\mathbf{C}(t)$, and $\mathbf{D}(t)$. Note that the rotation path also defines a contact path (but we will refer to it as a rotation path instead throughout the paper). These contact define the boundary of the shape as seen in figure 3 below from Romik's paper.

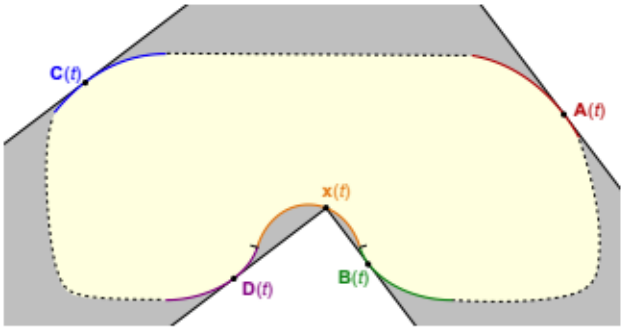

Figure 3: The contact points and contact paths

To roughly summarize the rest of Romik's paper, he was able to find necessary conditions that, under some assumptions, the contact paths must meet for them to define the maximal area shape which can traverse the hallway. Since the contact paths are uniquely determined by the rotation path, these necessary conditions for the contact paths implies necessary conditions for the rotation path. From these observations, Romik was able to derive a rotation path which produced a locally optimal solution which produced results identical to Gerver's 1992 conjecture.

4 The Problem of Global Optimality and a Potential Solution

While there have been many proposed solutions to the moving sofa problem, none of them have been proven to be the global optimal. In fact, it's not even known whether the solution to the moving sofa problem is unique. It could be the case that there is a solution to the moving sofa problem which does not have horizontal symmetry, implying the existence of two solutions. It also remains to be proven whether Gerver's construction has area equal to the global optimal. This is what remains to be proven for the moving sofa problem to be considered "closed". How can we use the tools laid out by previous researchers to find the global optimal?

The answer may be found in a modified version of the moving sofa problem. Moser's statement assumes a 90-degree bend in the hallway. If we modify the hallway by "opening" it up so that it has a 0-degree bend (or no bend) then the global optimal is found at the function $\mathbf{x}(t) = (0, 0)^T$. In this case, the optimal solution is a unit wide and however long the hallway is. How does the optimal rotation path $\mathbf{x}$ change as a function of α the bend of

the hallway? Going forward we will discuss the bend of the hallway in terms of α expressed in radians. Furthermore, what can we say about optimal solutions (global or local) as a function of α?

5 Generalized Contact Paths

Before we are able to study potential solutions to the modified moving sofa problem, we need to modify the tools of past researchers. Romik derived a set of equations which define the points of tangency between the hallway and any given sofa as it moves through the hallway. Embedded in Romik's proof was the assumption that $\alpha = \pi/2$. We will modify his proof by taking out this assumption and replacing it with a parameter which defines the angle of the hallway. Before we define our modified contact paths, we need to define two separate orthonormal basis which will be used throughout the paper. The first set is defined as follows

$$\mathbf{u}_t = \begin{pmatrix} \cos t \\ \sin t \end{pmatrix} \quad \text{and} \quad \mathbf{v}_t = \begin{pmatrix} -\sin t \\ \cos t \end{pmatrix}$$

and the second set is given by

$$\mathbf{q}_t = \cos\alpha \mathbf{u}_t + \sin\alpha \mathbf{v}_t \quad \text{and} \quad \mathbf{r}_t = -\sin\alpha \mathbf{u}_t + \cos\alpha \mathbf{v}_t$$

The basis **u,v** gives us our normal basis vectors $(1, 0)$ and $(0, 1)$ rotated around the plane. The basis **q,r** give us the same thing, just pre-rotated by α radians.

Theorem 5.1. *Let $\boldsymbol{x} : [0, \pi/2] \to \mathbb{R}^2$ be differentiable for all values of t in the interval. Also, assume that $\boldsymbol{x}$ is once differentiable and that each of the contact points are differentiable at all but a finite number of points. Then, the following relations describe the contact paths as a function of $\boldsymbol{x}$.*

$$\boldsymbol{A}(t) = \boldsymbol{x}(t) + \langle \boldsymbol{x}'(t), \boldsymbol{u}_t \rangle \boldsymbol{v}_t + \boldsymbol{u}_t \tag{1}$$
$$\boldsymbol{B}(t) = \boldsymbol{x}(t) + \langle \boldsymbol{x}'(t), \boldsymbol{u}_t \rangle \boldsymbol{v}_t \tag{2}$$
$$\boldsymbol{C}(t) = \boldsymbol{x}(t) + \langle \boldsymbol{x}'(t), \boldsymbol{q}_t \rangle \boldsymbol{r}_t + \boldsymbol{q}_t \tag{3}$$
$$\boldsymbol{D}(t) = \boldsymbol{x}(t) + \langle \boldsymbol{x}'(t), \boldsymbol{q}_t \rangle \boldsymbol{r}_t \tag{4}$$

Proof. By definition, we know that $\mathbf{C}(t)$ must lie on the line l_t defined by

$$l_t := \{\mathbf{p} \in \mathbb{R}^2 | \langle \mathbf{p}, \mathbf{q}_t \rangle\} = \langle \mathbf{x}(t), \mathbf{q}_t \rangle + 1$$

where $\langle \cdot, \cdot \rangle$ denotes the inner product. Let $s = t + \delta$ for $\delta > 0$ a small real. Let $\mathbf{p}(s, t)$ be the intersection of lines l_s, l_t. By the continuity assumption of the contact paths, we know that

$$\lim_{\delta \to 0} \mathbf{p}(s, t) = \mathbf{C}(t)$$

Recall that the contact path $\mathbf{C}(t)$ is defined as the point of tangency on the outer wall of the upper arm of the hallway (defined by the **q**,**r** base). Since each arm of the hallway is of unit width, by the definition of $\mathbf{C}(t)$ the following must hold.

$$\langle \mathbf{p}(s, t), \mathbf{q}_t \rangle = \langle \mathbf{x}(t), \mathbf{q}_t \rangle + 1 \tag{5}$$

$$\langle \mathbf{p}(s,t), \mathbf{q}_s \rangle = \langle \mathbf{x}(s), \mathbf{q}_s \rangle + 1 \tag{6}$$

By expanding the identity for q_s given right before the theorem statement we obtain the expression

$$\cos(\alpha)\langle \mathbf{p}(s,t), \mathbf{u}_s \rangle = -\sin(\alpha)\langle \mathbf{p}(s,t), \mathbf{v}_s \rangle + \langle \mathbf{x}(t), \mathbf{q}_s \rangle + 1$$

Now, note that $\mathbf{u}_s = \cos(\delta)\mathbf{u}_t + \sin(\delta)\mathbf{v}_t$ and similarly $\mathbf{v}_s = \cos(\delta)\mathbf{v}_t - \sin(\delta)\mathbf{u}_t$. Substitute these new forms in to the expression to obtain

$$\begin{aligned}\cos(\alpha)\langle \mathbf{p}(s,t), \cos(\delta)\mathbf{u}_t \rangle + \cos(\alpha)\langle \mathbf{p}(s,t), \sin(\delta)\mathbf{v}_t \rangle = \\ -\sin(\alpha)\langle \mathbf{p}(s,t), \cos(\delta)\mathbf{v}_t \rangle + \sin(\alpha)\langle \mathbf{p}(s,t), \sin(\delta)\mathbf{u}_t \rangle \\ + \langle \mathbf{x}(t), \mathbf{q}_s \rangle + 1\end{aligned}$$

Using our identities for q, r we can simplify the expression to

$$\cos(\alpha)\cos(\delta)\langle \mathbf{p}(s,t), \mathbf{u}_t \rangle + \sin(\delta)\langle \mathbf{p}(s,t), \mathbf{r}_t \rangle = -\sin(\alpha)\cos(\delta)\langle \mathbf{p}(s,t), \mathbf{v}_t \rangle + \langle \mathbf{x}(t), \mathbf{q}_s \rangle + 1$$

A bit more

$$\cos(\delta)\langle \mathbf{p}(s,t), \mathbf{q}_t \rangle + \sin(\delta)\langle \mathbf{p}(s,t), \mathbf{r}_t \rangle = \langle \mathbf{x}(s), \mathbf{q}_s \rangle + 1$$

We plug in (5) to get a projection of $\mathbf{p}$ purely in terms of one of the basis vectors. After some simplification we divide by the entire expression by $\delta \to 0$ and arrive at the projection

$$\langle \mathbf{C}(t), \mathbf{r}_t \rangle = \langle \mathbf{x}'(t), \mathbf{q}_t \rangle + \langle \mathbf{x}(t), \mathbf{r}_t \rangle$$

We established at the beginning of the proof, in equation (5), that

$$\langle \mathbf{p}(s,t), \mathbf{q}_t \rangle = \langle \mathbf{x}(t), \mathbf{q}_t \rangle + 1 \implies \langle \mathbf{C}(t), \mathbf{q}_t \rangle = \langle \mathbf{x}(t), \mathbf{q}_t \rangle + 1$$

These two equations give the orthonormal projections of $\mathbf{C}(t)$ in the directions of $\mathbf{r}_t$ and $\mathbf{q}_t$. A quick check of the proposed expression in (3) for $\mathbf{C}(t)$ shows that this is indeed the correct expression. This check is done by taking the dot product of $\mathbf{C}(t)$ with $\mathbf{q}_t$ and $\mathbf{r}_t$ and noticing that the proposed solution gives these projections. The remaining proofs are nearly identical, and so they are omitted. □

6 A Family of Differential Equations

With contact paths generalized to any hallway with bend α, we can correctly map any rotation path $\mathbf{x}(t)$ to its resulting sofa shape $S_{\mathbf{x}}$. However, derivation doesn't immediately give an obvious method for searching all possible rotation paths for the maximum. Recall Gerver's balanced condition which was the discrete equivalent of saying that the maximum sofa cannot increase in size when its boundary undergoes slight perturbations. By implementing the continuous version of Gerver's argument we are able to derive a set of differential equations that the rotation path $\mathbf{x}(t)$ must satisfy in order for the resulting shape $S_{\mathbf{x}}$ to be the maximum under perturbations of $\mathbf{x}(t)$. The following lemma is a preliminary result which helps simplify the presentation of the differential equations and makes them easier to solve.

Lemma 6.1. *Let $\boldsymbol{y}(t) = R_{-t}\boldsymbol{x}'(t)$. Let the orthogonal projections of $\boldsymbol{x}''(t)$ be given by*

$$\langle \boldsymbol{x}''(t), \boldsymbol{u}_t \rangle = c_1 \langle \boldsymbol{x}'(t), \boldsymbol{u}_t \rangle + c_2 \langle \boldsymbol{x}'(t), \boldsymbol{v}_t \rangle - v_1$$
$$\langle \boldsymbol{x}''(t), \boldsymbol{v}_t \rangle = c_3 \langle \boldsymbol{x}'(t), \boldsymbol{u}_t \rangle + c_4 \langle \boldsymbol{x}'(t), \boldsymbol{v}_t \rangle - v_2$$

Then, the expression for $\boldsymbol{x}''(t)$ is equivalently given by $\boldsymbol{y}'(t) = T\boldsymbol{y}(t) + \boldsymbol{v}$ with

$$T = \begin{pmatrix} c_1 & c_2 + 1 \\ c_3 - 1 & c_4 \end{pmatrix} \quad \text{and} \quad \boldsymbol{v} = \begin{pmatrix} v_1 \\ v_2 \end{pmatrix}$$

Proof. Using the substitution $\mathbf{y}(t) = R_{-t}\mathbf{x}'(t)$, the expression $\mathbf{y}'(t) = T\mathbf{y}(t) + \mathbf{v}$ becomes

$$R_{-t}\mathbf{x}''(t) - R'_{-t}\mathbf{x}'(t) = TR_{-t} + \mathbf{x}'(t) + \mathbf{v}$$

With just a bit of algebra, this expression becomes

$$\mathbf{x}''(t) = R_t\Big((TR_{-t} + R'_{-t})\mathbf{x}'(t) + \mathbf{v}\Big)$$

If we let

$$T = \begin{pmatrix} t_1 & t_2 \\ t_3 & t_4 \end{pmatrix}$$

and notice that the equality has to hold because of the orthonormal projections

$$TR_{-t} + R'_{-t} = \begin{pmatrix} c_1 \cos t - c_2 \sin t & c_1 \sin t + c_2 \cos t \\ c_3 \cos t - c_4 \sin t & c_3 \sin t + c_4 \cos t \end{pmatrix}$$

Then with some algebra we get

$$T = \begin{pmatrix} c_1 & c_2 + 1 \\ c_3 - 1 & c_4 \end{pmatrix}$$

which completes the proof. □

Now we know that if we can find an orthogonal expression for the second derivative of the rotation path that we can express it as a simple first order system. Now we can move to find the differential equations which $\mathbf{x}$ must satisfy for it to map to the solution to the moving sofa problem.

Theorem 6.2. *Let $\boldsymbol{x}$ be the usual rotation path. We say $\boldsymbol{x}$ is well-behaved at t if $\boldsymbol{x}$ is twice continuously differentiable at t and the following hold:*

1. *If $\boldsymbol{x}(t)$ is a contact point, then $\langle \boldsymbol{x}'(t), \boldsymbol{v}_t \rangle \geq 0$ and $\langle \boldsymbol{x}'(t), \boldsymbol{u}_t \rangle \leq 0$.*
2. *If $\boldsymbol{A}(t)$ is defined then $\langle \boldsymbol{A}'(t), \boldsymbol{q}_t \rangle \geq 0$*
3. *If $\boldsymbol{B}(t)$ is defined then $\langle \boldsymbol{B}'(t), \boldsymbol{q}_t \rangle \leq 0$*
4. *If $\boldsymbol{C}(t)$ is defined then $\langle \boldsymbol{C}'(t), \boldsymbol{u}_t \rangle \leq 0$*
5. *If $\boldsymbol{D}(t)$ is defined then $\langle \boldsymbol{D}'(t), \boldsymbol{u}_t \rangle \geq 0$*

Then, assume that $\boldsymbol{x}$ *is well-behaved. Let* $\Gamma_{\boldsymbol{x}}$ *define the set of contact points currently present for some value of* t*. Note that not all contact points need to be defined for any particular value of* t *which is the motivation for considering particular sets of present contact points. If* $\boldsymbol{x}$ *is the rotation path associated with a solution to the moving sofa problem then at any given* t*,* $\boldsymbol{x}$ *must satisfy one of the following differential equations.*

- ***Case 1:*** $\Gamma_x = \{\boldsymbol{A}, \boldsymbol{C}, \boldsymbol{D}\}$

$$\boldsymbol{y}'(t) = \begin{pmatrix} 0 & -1 \\ 1 & 0 \end{pmatrix} \boldsymbol{y}(t) + \begin{pmatrix} -1 \\ \cot\alpha - 1/2 \sin^{-1}\alpha \end{pmatrix} \tag{7}$$

- ***Case 2:*** $\Gamma_x = \{\boldsymbol{x}, \boldsymbol{A}, \boldsymbol{C}, \boldsymbol{D}\}$

$$\boldsymbol{y}'(t) = \begin{pmatrix} \cot\alpha & 0 \\ 1/2 \sin^{-2}\alpha - 3\cot^2\alpha & -\cot\alpha \end{pmatrix} \boldsymbol{y}(t) + \begin{pmatrix} -1 \\ \cot\alpha - 1/2 \sin^{-1}\alpha \end{pmatrix} \tag{8}$$

- ***Case 3:*** $\Gamma_x = \{\boldsymbol{x}, \boldsymbol{A}, \boldsymbol{C}\}$

$$\boldsymbol{y}'(t) = \begin{pmatrix} \cot\alpha & 0 \\ -2\cot^2\alpha & -\cot\alpha \end{pmatrix} \boldsymbol{y}(t) + \begin{pmatrix} -1 \\ \cot\alpha - \sin^{-1}\alpha \end{pmatrix} \tag{9}$$

- ***Case 4:*** $\Gamma_x = \{\boldsymbol{x}, \boldsymbol{A}, \boldsymbol{B}, \boldsymbol{C}\}$

$$\boldsymbol{y}'(t) = \begin{pmatrix} 1/2\cot\alpha & -1/2 \\ -3/2\cot^2\alpha & -1/2\cot\alpha \end{pmatrix} \boldsymbol{y}(t) + \begin{pmatrix} -1/2 \\ 1/2\cot\alpha - \sin^{-1}\alpha \end{pmatrix} \tag{10}$$

- ***Case 5:*** $\Gamma_x = \{\boldsymbol{A}, \boldsymbol{B}, \boldsymbol{C}\}$

$$\boldsymbol{y}'(t) = \begin{pmatrix} 0 & -1 \\ 1 & 0 \end{pmatrix} \boldsymbol{y}(t) + \begin{pmatrix} -1/2 \\ 1/2\cot\alpha - \csc\alpha \end{pmatrix} \tag{11}$$

- ***Case 6:*** $\Gamma_x = \{\boldsymbol{x}, \boldsymbol{A}, \boldsymbol{B}, \boldsymbol{C}, \boldsymbol{D}\}$

$$\boldsymbol{y}'(t) = \begin{pmatrix} 1/2\cot\alpha & -1/2 \\ 1/2\sin^{-2}\alpha - 3/2\cot^2\alpha & -1/2\cot\alpha \end{pmatrix} \boldsymbol{y}(t) + \begin{pmatrix} -1/2 \\ 1/2\cot\alpha - 1/2\sin^{-1}\alpha \end{pmatrix} \tag{12}$$

Proof. Fix a small positive value δ, and denote $t' = t + \delta$. We replace Gerver's iterative balanced condition with the following sequence. We call $\mathbf{x}$ along its entire range the rotation path, and for any fixed value we call $\mathbf{x}$ the rotation point. We will consider the case for $\Gamma_x = \{\mathbf{x}, \mathbf{A}, \mathbf{C}\}$ in detail below.

1. As a time coordinate s ranges in $[0, t]$, drag the rotation point along the rotation path $\mathbf{x}(s)$ while rotating the hallway around that corner at an angle of s.

2. Slide the hallway without rotating it by a distance of δ in the direction of the vector $-r_t$.

3. As $s \in [t, t']$, drag the rotation point, now positioned at $x(t) - \delta r_t$, along $\mathbf{x}(s) - \delta \mathbf{r}_t$ for $s \in [t, t']$ while continuing rotation.

4. Slide the hallway back in direction of $\mathbf{r}_t$ by amount δ. The rotation point is now at position $\mathbf{x}(t')$.

5. Finish movement along the rest of the rotation path, $\mathbf{x}(s)$ for $s \in [t', \pi/2]$.

Let S_x be a sofa, and S'_x be the result of perturbing the rotation path of S_x as described above. Let λ be the area function of the plane. Notice that when we perform the perturbation sequence on S_x there is some amount of area lost near $x(t)$ and some amount gained near $A(t)$. This fact will be the focal point of our study. Also, note that no area was lost around $C(t)$. This is because $\mathbf{C}(t)$ is defined by the line of tangency to S_x is parallel to r_t and so the position of $C(t)$ was not changed.

The area lost around $x(t)$ is well approximated by a parallelogram with sides represented by vectors $\delta x'(t)$ and δr_t incident to $x(t)$. This gives us an area approximation of

$$\delta^2 \langle x'(t), q_t \rangle + o(\delta^2) \qquad (\delta \to 0)$$

Since $A'(t)$ is parallel to q_t, we approximate the area gained in the same way.

$$\delta^2 \langle A'(t), q_t \rangle + o(\delta^2) \qquad (\delta \to 0)$$

Assume that S_x is the optimal sofa. Under area maximizing assumptions, the following must hold

$$\langle x'(t) - A'(t), q_t \rangle \geq 0$$

If we push in direction r_t instead, still with the area maximization assumption, we get

$$\langle x'(t) - A'(t), q_t \rangle \leq 0$$

So we know that

$$\langle x'(t) - A'(t), q_t \rangle = 0$$

must hold.

We do something similar for the contact point C. We push in the direction of v_t by amount δ. This results in just a small modification of our perturbation sequence for steps 2 and 4. We get the expressions

$$\begin{aligned} \delta^2 \langle x'(t), u_t \rangle + o(\delta^2) \quad &\leftarrow \text{Area around x(t)} \\ \delta^2 \langle C'(t), u_t \rangle + o(\delta^2) \quad &\leftarrow \text{Area around C(t)} \end{aligned}$$

Then by the exact same methods above we get that

$$\langle x'(t) - C'(t), u_t \rangle = 0$$

must hold.

This leaves us with two facts about the contact points

$$\langle x'(t) - C'(t), u_t \rangle = 0 \tag{13}$$
$$\langle x'(t) - A'(t), q_t \rangle = 0 \tag{14}$$

Recall that we have expressions for A, C purely in terms of x. We also have expressions for q_t, r_t in terms of u_t, v_t. We will use these facts to derive an expression for $x''(t)$.

Note that (12) can be expressed as

$$\cos\alpha\langle x'(t) - A'(t), u_t\rangle + \sin\alpha\langle x'(t) - A'(t), v_t\rangle = 0$$

Differentiate the contact point A with respect to t to get

$$A'(t) = x'(t) + \langle x''(t), u_t\rangle v_t + \langle x'(t), v_t\rangle v_t - \langle x'(t), u_t\rangle u_t + v_t$$

Pug this into (12) in its expanded form to get

$$\cos\alpha\langle\langle x'(t), u_t\rangle, u_t\rangle + \sin\alpha\langle -\langle x''(t), u_t\rangle v_t - \langle x'(t), v_t\rangle v_t - \langle v_t, v_t\rangle = 0$$

Simplification gives an expression of x'' in terms of u_t

$$\langle x''(t), u_t\rangle = \cot\alpha\langle x'(t), u_t\rangle - \langle x'(t), v_t\rangle - 1 \tag{15}$$

A similar approach is taken to find $\langle \mathbf{x}''(t), \mathbf{v}_t\rangle$ giving us a set of orthonormal expressions for the second derivative of the rotation path.

$$\langle \mathbf{x}''(t), \mathbf{u}_t\rangle = \cot\alpha\langle \mathbf{x}'(t), \mathbf{u}_t\rangle - \langle \mathbf{x}'(t), \mathbf{v}_t\rangle - 1 \tag{16}$$
$$\langle \mathbf{x}''(t), \mathbf{v}_t\rangle = (1 - 2\cot^2\alpha)\langle \mathbf{x'}(t), \mathbf{u}_t\rangle - \cot\alpha\langle \mathbf{x}'(t), \mathbf{v}_t\rangle + (\cot\alpha - \sin^{-1}\alpha) \tag{17}$$

Which naturally leads to the differential equation

$$x''(t) = R_t\left(\begin{pmatrix} -1 \\ \cot\alpha - 1/\sin\alpha \end{pmatrix} + \begin{pmatrix} \cot\alpha\cos t + \sin t & \cot\alpha\sin t - \cos t \\ -\cot\alpha\sin t + \cos t & \cot\alpha\cos t + \sin t \end{pmatrix} x'(t)\right) \tag{18}$$

Let $\mathbf{y} = R_{-t}\mathbf{x}'(t)$. Then, the differential equation $\mathbf{y}'(t) = T\mathbf{y}(t) + \mathbf{v}$ is equivalent to (24) when

$$T = \begin{pmatrix} \cot\alpha & 0 \\ -2\cot^2\alpha & -\cot\alpha \end{pmatrix} \quad \text{and} \quad \mathbf{v} = \begin{pmatrix} -1 \\ \cot\alpha - \sin^{-1}\alpha \end{pmatrix}$$

This completes the proof for $\Gamma_x = \{\mathbf{x}, \mathbf{A}, \mathbf{C}\}$.

The proof of each case is similar, but requires a different set of starting assumptions which we will lay out and briefly discuss for each additional case before concluding the proof. Consider case 1 $\Gamma_x = \{\mathbf{A}, \mathbf{C}, \mathbf{D}\}$. By similar arguments as made before, since the area gained or lost near $\mathbf{C}(t)$ and $\mathbf{D}(t)$, due to a small perturbation of $\mathbf{x}(t)$ in the direction of $\mathbf{v}_t$ and $-\mathbf{v}_t$, must sum to zero then

$$\langle \mathbf{C}'(t) + \mathbf{D}'_t, \mathbf{u}_t\rangle = 0$$

must hold. Now for perturbations of $\mathbf{x}(t)$ in the direction of $\mathbf{r}_t$ and $-\mathbf{r}_t$ the area around the point $\mathbf{A}(t)$ must stay constant. This give that

$$\langle \mathbf{A}'(t), \mathbf{q}_t \rangle = 0$$

must hold. Since $\mathbf{A}'(t)$ is parallel to $\mathbf{q}_t$, if $\langle \mathbf{A}'(t), \mathbf{q}_t \rangle = 0$ it must be the case that $\mathbf{A}'(t) = 0$. This is the same as $\mathbf{A}(t)$ staying fixed in a small region of t. In this small region, $\mathbf{A}(t)$ would appropriately be named a *hinged point* where it is as if the hallway ceases simultaneous translation and rotation and for a moment rotates around $\mathbf{A}(t)$ with no translation. Using the methods demonstrated for the case $\Gamma_x\{\mathbf{x}, \mathbf{A}, \mathbf{C}\}$ we can use these inner product expressions to derive orthogonal expressions for $\mathbf{x}''$.

Now consider case 2 $\Gamma_x = \{\mathbf{x}, \mathbf{A}, \mathbf{C}, \mathbf{D}\}$. Again, we consider perturbations in the directions of $\pm\mathbf{v}_t$ and $\pm\mathbf{r}_t$. This leads to the expressions

$$\langle \mathbf{x}'(t) - \mathbf{A}'(t), \mathbf{q}_t \rangle = 0$$

for perturbations in the direction of $\pm\mathbf{r}_t$. For the case of perturbations in the direction of $\pm\mathbf{v}_t$ we have to consider area gained and lost at three points now: $\mathbf{D}$, $\mathbf{C}$, and $\mathbf{x}$. This leads to the condition that

$$\langle \mathbf{x}'(t) - \mathbf{C}'(t) - \mathbf{D}'(t), \mathbf{u}_t \rangle = 0$$

For case 4 $\Gamma_x = \{\mathbf{x}, \mathbf{A}, \mathbf{B}, \mathbf{C}\}$ the setup is conceptually identical. We end with the expressions

$$\langle \mathbf{x}'(t) - \mathbf{C}'(t), \mathbf{u}_t \rangle = 0$$

for the perturbations in the direction of $\pm\mathbf{v}_t$ and

$$\langle \mathbf{x'}(t) - \mathbf{A}'(t) - \mathbf{B}'(t), \mathbf{q}_t \rangle = 0$$

for perturbations in the direction of $\pm\mathbf{r}_t$.

For case 5 $\Gamma_x = \{\mathbf{A}, \mathbf{B}, \mathbf{C}\}$ we get the expressions

$$\langle textbf A'(t) + \mathbf{B}'(t), \mathbf{q}_t \rangle = 0$$

and

$$\langle \mathbf{C}'(t), \mathbf{u}_t \rangle = 0$$

which shows that $C(t)$ is a hinge point.

Finally, for case 6 $\Gamma_x = \{\mathbf{x}, \mathbf{A}, \mathbf{B}, \mathbf{C}, \mathbf{D}\}$ we get the expressions

$$\langle \mathbf{x}'(t) - \mathbf{A}'(t) - \mathbf{B}'(t), \mathbf{u}_t \rangle = 0$$

and also

$$\langle \mathbf{x}'(t) - \mathbf{C}'(t) - \mathbf{D}'(t), \mathbf{u}_t \rangle = 0$$

Note that cases like $\Gamma_x = \{\mathbf{x}, \mathbf{B}, \mathbf{D}\}$ cannot exist under the assumption that the sofa has maximum area. This is because a perturbation of $\mathbf{x}$ in the direction of $\pm\mathbf{r}_t \pm \mathbf{v}_t$ will always have a strictly area increasing or decreasing effect on S. This is the case for all combinations of contact points not represented in the six cases.

This proves that under the assumption that the shape $S_{\mathbf{x}}$ is the maximum area sofa, the family of the six differential equations must hold. □

6.1 Solving the Family of Differential Equations

Now we have the task of solving each of these differential equations. Luckily, the substitution $\mathbf{y}(t) = R_{-t}\mathbf{x}'(t)$ serves as a way to simplify the computation along with simplifying the presentation. Note that all of our differential equations are now first order in the form $\mathbf{y}(t) = A\mathbf{y}(t)+\mathbf{v}$ where A is a constant matrix and v a constant vector. For all six differential equations we can write $A = PDP^{-1}$ where P is invertible and D is diagonal. This allows us to use decoupling by further making the substitution $\mathbf{y}(t) = P\mathbf{u}(t)$ and writing

$$\mathbf{u}'(t) = D\mathbf{u}(t) + P^{-1}\mathbf{v} \tag{19}$$

This system is easily solved via variation of constants. The solution for $\mathbf{u}(t)$ follows the usual form.

$$\mathbf{u}(t) = e^{Dt}\begin{pmatrix} c_1 \\ c_2 \end{pmatrix} + \int^t e^{(t-s)D}P^{-1}\mathbf{v}ds \tag{20}$$

By multiplying $\mathbf{u}(t)$ by P we obtain our expression for $\mathbf{y}(t)$.

$$P\mathbf{u}(t) = \mathbf{y}(t) = Pe^{Dt}\begin{pmatrix} c_1 \\ c_2 \end{pmatrix} - Pe^{Dt}D^{-1}e^{-Dt}P^{-1}\mathbf{v} \tag{21}$$

Since $\mathbf{y}(t) = R_{-t}\mathbf{x}'(t)$, we'll multiply by R_t to get an expression for $\mathbf{x}'(t)$.

$$\mathbf{x}'(t) = R_tP\big(e^{Dt}\begin{pmatrix} c_1 \\ c_2 \end{pmatrix} - e^{Dt}D^{-1}e^{-Dt}P^{-1}\mathbf{v}\big) \tag{22}$$

Theorem 6.3 (ODE Solutions)**.** *The set of solutions to the family of differential equations is given piecewise for each of the equations. Cases 2,3,4 are singular for $\alpha = \pi/2$ and have to be solved differently for the $\pi/2$ case. This is almost certainly due to the fact that the rotation path obtains an inflection point for $\alpha = \pi/2$ case just as $\sqrt{1-x^2}$ does when $x = 1$. Case 6 is singular for $\alpha = \pi/3$ and $\alpha = 2\pi/3$. What makes this a special point is not immediately clear. The solutions for the differential equations are given below. Note that the solutions*

for $\alpha = \pi/2$ are given by Dan Romik.

$$\boldsymbol{x}_1(t) = R_t \begin{pmatrix} e_1 \cos t + e_2 \sin t - 1 \\ \\ -e_2 \cos t + e_1 \sin t + \cot \alpha - 1/2 \csc \alpha \end{pmatrix} + \boldsymbol{k}_1$$

$$\boldsymbol{x}_2(t) = \begin{cases} R_t \begin{pmatrix} -3 + \dfrac{\csc^2 \alpha}{2a^2} + \dfrac{f_2}{a^2+1} e^{-at} + \dfrac{f_1/(4a) \csc^2 \alpha - 1/2 a f_1}{a^2+1} e^{at} \\ \\ -\dfrac{1}{a} - \dfrac{f_1}{a^2+1} e^{at} - f_2 \dfrac{a}{a^2+1} e^{-at} + \dfrac{f_1/4 \csc^2 \alpha - 3/2 a^2 f_1}{a^2+1} e^{at} \end{pmatrix} + \boldsymbol{k}_2 & \alpha \neq \pi/2 \\ \\ R_t \begin{pmatrix} -\dfrac{1}{4} t^2 + f_1 t + f_2 \\ \\ \dfrac{1}{2} t - f_1 - 1 \end{pmatrix} + \boldsymbol{k}_2 & \alpha = \pi/2 \end{cases}$$

$$\boldsymbol{x}_3(t) = \begin{cases} R_t \begin{pmatrix} g_1 e^{-at} \big(\dfrac{1}{a^2+1} \big) + \dfrac{\csc \alpha - a}{2a^2 - a} \\ \\ g_2 e^{at} \big(\dfrac{1+a^2}{a^3+a} \big) - g_1 e^{-at} \big(\dfrac{a}{a^2+1} \big) - \dfrac{1}{a} \end{pmatrix} + \boldsymbol{k}_3 & \alpha \neq \pi/2 \\ \\ R_t \begin{pmatrix} g_1 - t \\ g_2 + t \end{pmatrix} + \boldsymbol{k}_3 & \alpha = \pi/2 \end{cases}$$

$$\boldsymbol{x}_4(t) = \begin{cases} R_t \begin{pmatrix} h_1 \dfrac{2}{3a^2+3} e^{-at} - \big(\dfrac{1}{2} + \dfrac{\csc \alpha}{2a} \big) \\ \\ h_2 \dfrac{1}{a} e^{at} - h_1 e^{-at} \dfrac{1+3a^2}{3a^3+3a} - \big(\dfrac{1}{2a} - \dfrac{\csc \alpha}{2a^2} \big) \end{pmatrix} + \boldsymbol{k}_4 & \alpha \neq \pi/2 \\ \\ R_t \begin{pmatrix} -\dfrac{1}{2} t + h_1 - 1 \\ \\ -\dfrac{1}{4} t^2 + h_1 t + h_2 \end{pmatrix} + \boldsymbol{k}_4 & \alpha = \pi/2 \end{cases}$$

$$\boldsymbol{x}_5(t) = R_t \begin{pmatrix} m_1 \cos t + m_2 \sin t - \dfrac{1}{2} \\ \\ -m_2 \cos t + m_1 \sin t + \dfrac{a}{2} - \csc \alpha \end{pmatrix} + \boldsymbol{k}_5$$

$$\boldsymbol{x}_6(t) = \begin{cases} R_t \begin{pmatrix} n_1 e^{-\sqrt{a^2-c}t}\left(\dfrac{a^2 - a\sqrt{a^2-c}}{ca^2 - c^2 + c}\right) + n_2 e^{\sqrt{a^2-c}t}\left(\dfrac{a^2 + a\sqrt{a^2-c}}{a^2 - c + 1}\right) + \dfrac{c + av_2}{a^2 - c} \\ \\ -n_1 e^{-\sqrt{a^2-c}t}\left(\dfrac{(c-1)\sqrt{a^2-c} + a}{ca^2 - c^2 + c}\right) - n_2 e^{\sqrt{a^2-c}t}\left(\dfrac{(1-c)\sqrt{a^2-c} + a}{a^2 - c + 1}\right) - \dfrac{a + v_2 - \sqrt{a^2-c}}{2a^2 - 2c} \end{pmatrix} \\ + \boldsymbol{k}_6 \\ R_t \begin{pmatrix} n_1 \cos(t/2) + n_2 \sin(t/2) - 1 \\ -n_2 \cos(t/2) + n_1 \sin(t/2) - 1 \end{pmatrix} + \boldsymbol{k}_6 \end{cases}$$

Where $a = \cot \alpha$, $b = 1/2 \csc^2 \alpha - 3 \cot^2 \alpha$ *and* $c = 3 - 2 \csc^2 \alpha$, *and* $e_i, f_i, g_i, h_i, m_i, n_i$ $(i = 1, 2)$ *are arbitrary constant real numbers. Also,* $\boldsymbol{k}_1, \boldsymbol{k}_2, \boldsymbol{k}_3, \boldsymbol{k}_4$, $\boldsymbol{k}_5$, *and* $\boldsymbol{k}_6$ *are constants in* $\mathbb{R}^2$.

Proof. These equations can be checked to be correct by first changing the variable to y and then plugging in to the given differential equations in theorem 6.2. The change of variables is simple. Notice that each of the equations is given in the form $\mathbf{x}_i(t) = R_t \chi(t) + \mathbf{k}_i$ a combination of a rotation term and a translation term. Then, by the definition of $\mathbf{y}(t) = R_{-t}\mathbf{x}'(t)$, we get the simple expression

$$\mathbf{y}(t) = \chi'(t) + \begin{pmatrix} 0 & -1 \\ 1 & 0 \end{pmatrix} \chi(t)$$

which is easily plugged into the differential equations for verification. □

7 Numerically Optimizing Shapes in the Moving Sofa Problem

Gerver's Sofa is constructed by gluing together x_1, x_2, x_3, x_4, and x_5. This results in a five part piecewise equation with a whopping 20 unknown constants. In Romik's construction of Gerver's sofa, he overcame this obstacle by making a number of assumptions about the geometry of the resulting sofa. Many of these assumptions were able to be made because Romik already knew the geometry of Gerver's sofa as it had already been analytically constructed in Gerver's 1992 paper. In fact, even knowing the correct order for the rotation paths to be glued together in took some foreknowledge. Initially, this poses a substantial problem for deriving sofas for α not equal to $\pi/2$ as there are no explicit constructions of such shapes. Without previous geometric insights, there is no clear path to being able to whittle down the large number of unknown constants into a solvable system. Fortunately,

we can overcome this obstacle with numerics. As mentioned in the introduction, Gerver proved that a sequence of polygons could be constructed which would converge to a solution to the moving sofa problem. Using this fact, we can derive an algorithm written in Python3 which converges to Gerver's sofa with seemingly arbitrary accuracy. Further, we can use this algorithm to produce candidate solutions for the moving sofa problem when α is not equal to $\pi/2$. The following describes the basic process of the algorithm.

7.1 The Algorithm

1. Set the angle of the hallway α. In this description we'll define $L^{(\alpha)}$ as the hallway with a bend of angle α. Then, pass the program a "guess" for the optimal rotation path. While any path will do, the rotation path for Hammersley's sofa

$$x(t) = \Big(2/\pi \cos(2t) - 2/\pi, 2/\pi \sin(2t)\Big)$$

   will produce quick convergence to Gerver's sofa and produces a connected polygon for any angle $\alpha \leq 5\pi/6$ (possibly greater, too). This observation may be useful for anyone interested in reproducing the results of the algorithm.

2. For general values of $0 < \alpha < \pi$, the sofa $S_{\mathbf{x}}$ is defined as

$$S_{\mathbf{x}} = L^{(\alpha)}_{horiz} \cap \bigcap_{0 \leq t \leq \pi/2} \Big(x(t) + R_t(L^{(\alpha)})\Big) \cap \Big(x(\pi/2) + R_{\pi/2}(L^{(\alpha)}_{vert})\Big)$$

   We can approximate this shape by taking a finite number of intersections of the hallway as it rotates and translates accross the plane. Let N be the number of intersections (a measure of granularity) we wish to take. Redefine our time variable so that $t = \alpha \cdot n/N$. Then, our discrete approximation denoted $DS'_{\mathbf{x}}$ takes the form

$$DS_{\mathbf{x}} = L_{horiz} \cap \bigcap_{n=0}^{N} \Big(x(t) + R_t(L)\Big) \cap \Big(x(\pi/2) + R_{\pi/2}(L_{vert})\Big)$$

   Note: Things are kept simple programatically by keeping each of the hallway shapes as objects in an array where the hallway shape at index k would be the position of the hallway after being rotated and translated at time $\alpha \cdot k/N$. We intersect all of the hallway shapes and check the area of the resulting polygon when necessary. Shapely was used to manage polygonal intersections and for area calculations.

3. Now we optimize the discrete approximation. Select the k^{th} hallway out of the array. Perturb it by a small amount in the direction of $\mathbf{v}_t$. Intersect all of the hallway shapes and check the area of the resulting discrete approximation. If the area increased, we save this as the k^{th} hallway's new position. If the area decreased, we move the k^{th} hallway back to its original position and try the perturbation in the direction of $-\mathbf{v}_t$ instead. If neither perturbation resulted in an increase in area, we try perturbations in the directions of $\pm\mathbf{q}_t$. If none of the four perturbation directions result in an area increase, the program slightly decreases the variable which sets the magnitude of the

perturbation and moves to the $k + 1^{th}$ hallway and repeats the process. An graphical representation of a single perturbation step is shown below.

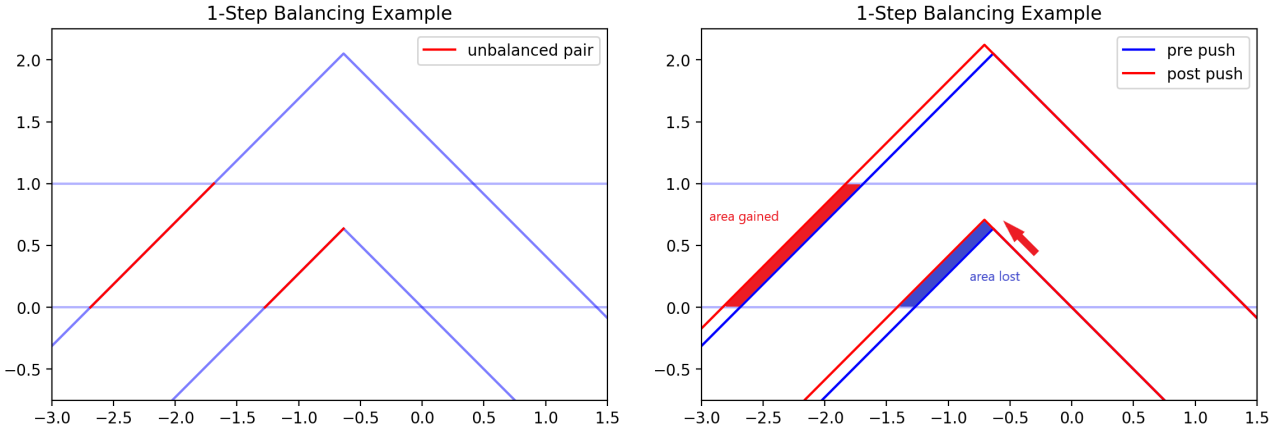

Figure 4: How Perturbations Increase Intersection Area

4. The program terminates when it has been unable to increase the area of the discrete approximation for a significant amount of time. Specifically, the program will try to make four entire cycles through the array of hallways before it gives up. This means that, since the program attempts four separate positional perturbations for each hallway in the array, that the program will make 4^{N+1} failed area increasing attempts before terminating.

5. After terminating, the program saves high resolution plots of the approximated maximum along with the initial position of the hallway.

The interior of the resulting polygon, where the rotation path would usually slide, is left with jagged edges as a product of the finite approximation. After terminating, the algorithm uses piecewise linear interpolation to smooth the interior edges of the polygon to increase accuracy. An example is shown below for $N = 8$ and $\alpha = \pi/2$. The faint colored outlines in the background are the outlines of the hallways which, when intersected, result in the shown polygon.

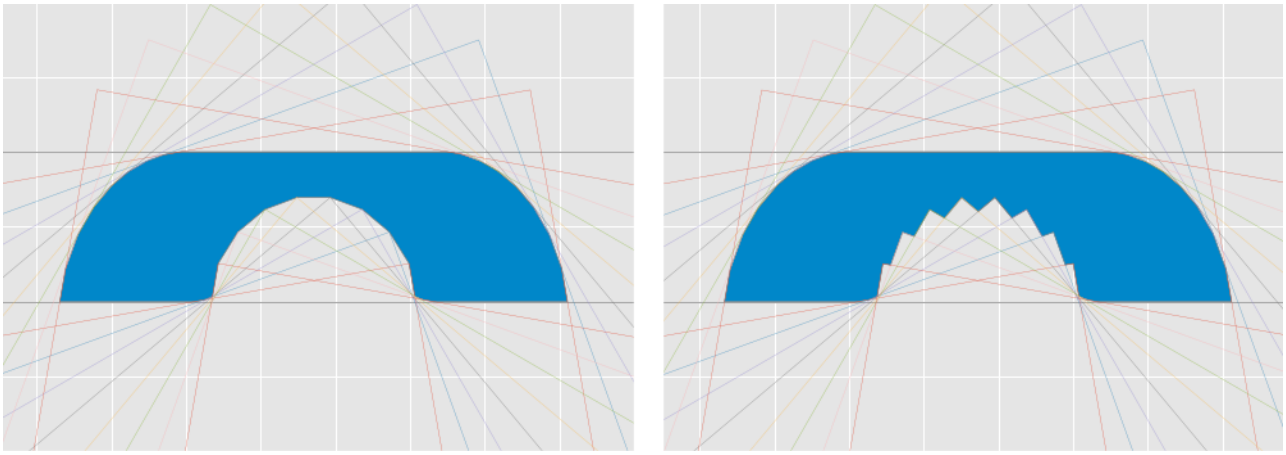

Figure 5: Smoothing of the Rotation Path for $\alpha = \pi/2$ and $N = 8$.

Already, a low value of N along with smoothing of the interior edges produces a discrete approximation which looks very similar to Gerver's sofa. To show that smoothing actually increases the rate of convergence we have the algorithm produce approximations for Gerver's sofa for values of $N \in \{5, 6, ..., 32\}$ and compare the approximated area to the true value. The results are in the loglog blow below.

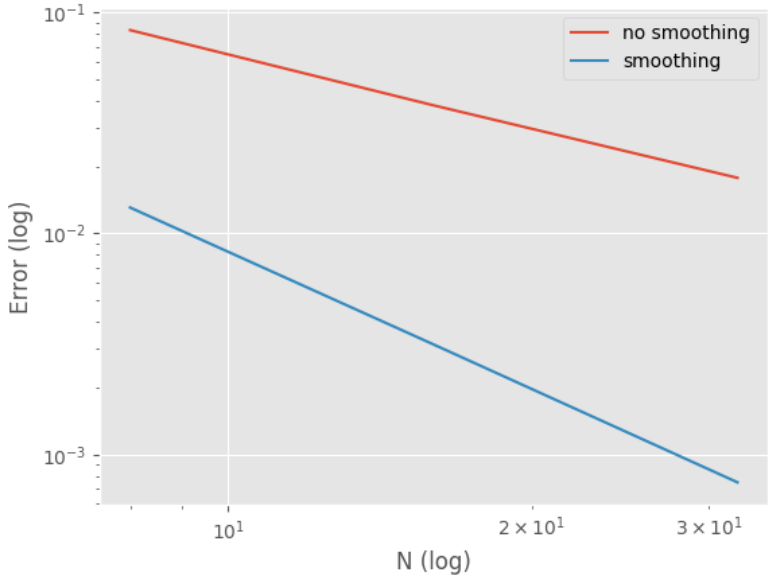

Figure 6: Accuracy of Discrete Approximations to Gerver's Sofa

For $N = 32$, a high accuracy and resolution approximation of Gerver's sofa was produced with an absolute area error of approximately 4×10^{-4} after piecewise linear smoothing. The approximation is shown in the figure below. The number at the top of the plot is the area and the value of N following "N:".

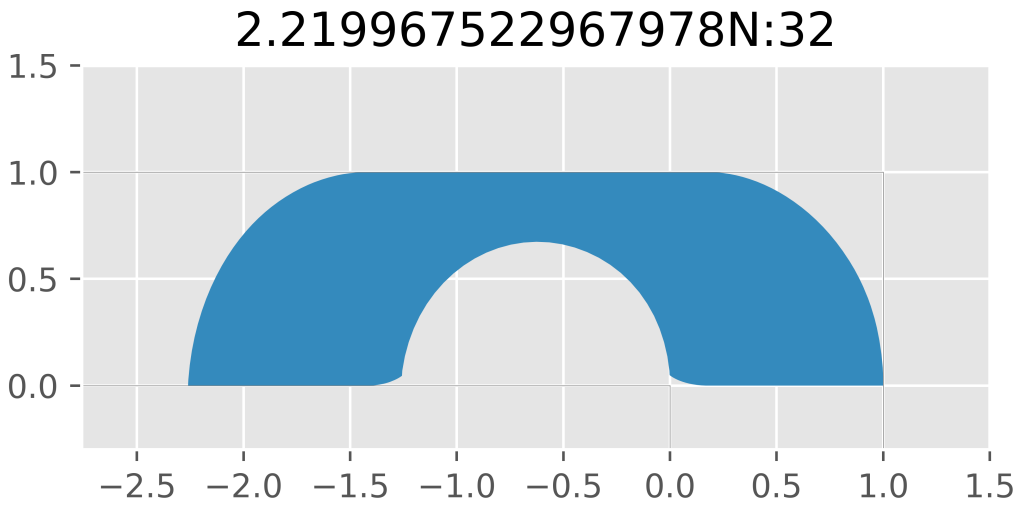

Figure 7: Discrete Approximation for Gerver's Sofa

If Gerver had not previously published the construction of his sofa we could use this discrete approximation to to conclude the correct order in which the rotation paths must be glued together to produce a candidate solution for the moving sofa problem when $\alpha = \pi/2$. We would also likely be able to make many of the assumptions that Romik made in order to simplify the system of 20 unknown constants. For example, Romik assumed that the rotation path A had an initial value of $A(0) = (1, 0)$ which is exactly what we see in figure 7. We can also plot the sofa with hallway outlines for different values of t to understand how the rotation path transitions between different tangency cases.

As seen in the figure below, the first tangency case begins at $t = 0$. Highlighted by red dots, we can see that the hallway is tangent to the sofa at points $\mathbf{A}, \mathbf{C}$, and $\mathbf{D}$. Notice that the rotation path $\mathbf{x}(t)$ is not defined at the outset. This corresponds to the rotation path $\mathbf{x}_1(t)$.

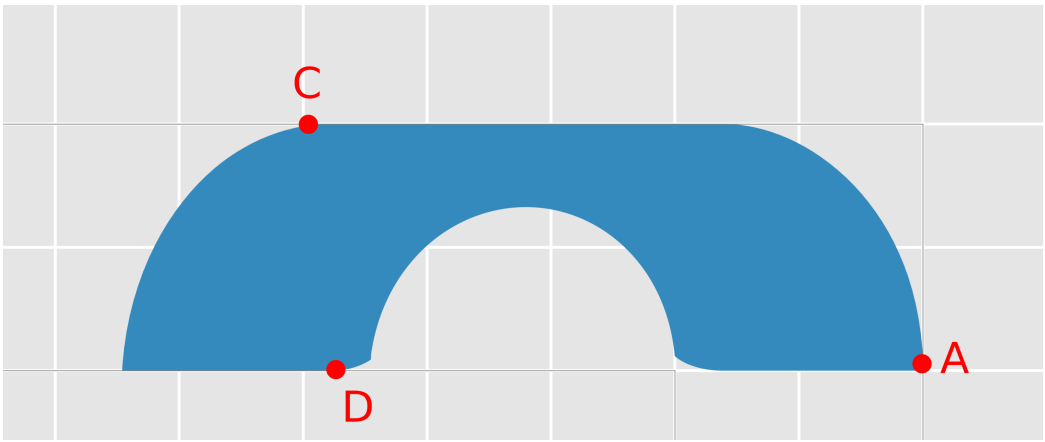

Figure 8: The Case of $\mathbf{x}_1(0)$

Next, we see that as the hallway rotates around, the previously defined points of tangency remain while the rotation path $\mathbf{x}(t)$ begins to touch the interior edge of the sofa. This corresponds to the rotation path $\mathbf{x}_2(t)$.

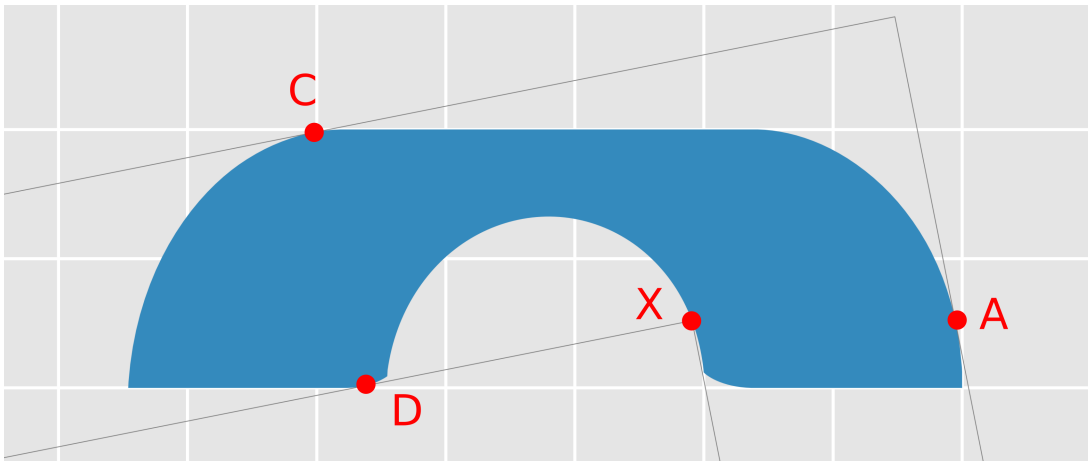

Figure 9: The Case of $\mathbf{x}_2(t)$

Then, as t tends towards the halfway points of $\pi/4$ the rotation point $\mathbf{D}$ no longer touches the sofa and so the rotation path $\mathbf{D}(t)$ is no longer defined.

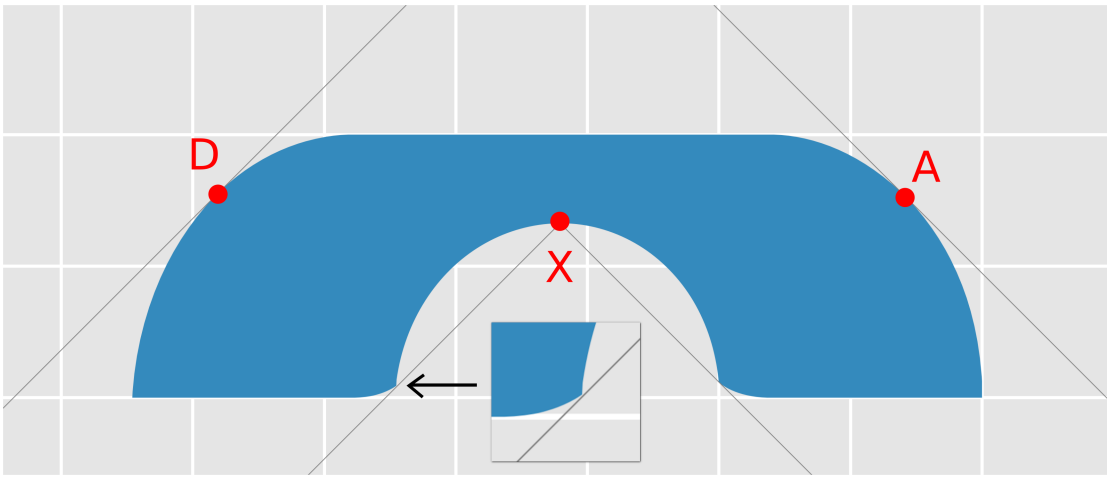

Figure 10: The Case of $\mathbf{x}_3(t)$ near $\pi/4$ with a small gap highlighted

The following two tangency cases are the horizontally symmetric version of the first two ($\mathbf{x}_4(t)$ and $\mathbf{x}_5(t)$ respectively) so their plots are omitted.

The amount of information we were able to gather about the $\alpha = \pi/2$ case by using the algorithm gives us reason to believe that for other values of α, the program will converge accurately to candidate solutions while providing us with enough insight into the geometry of the solution to be able to begin to solve for the 20 unknowns.

8 A Family of Solutions for $\alpha < \pi/2$

Now that we have a family of equations that describe the rotation path for different tangency cases and the tools to make the necessary insights into the geometry of potential solutions we are ready to derive new candidate solutions to the modified moving sofa problem. Arbitrarily, we'll construct a sofa for $\alpha = \pi/3$ first. Using the algorithm, we output images which let us identify the cases of tangency the shape transitions through. The first tangency case is given by $\{\mathbf{x}, \mathbf{A}, \mathbf{C}, \mathbf{D}\}$ which corresponds to $\mathbf{x}_2(t)$ as seen in figure 11.

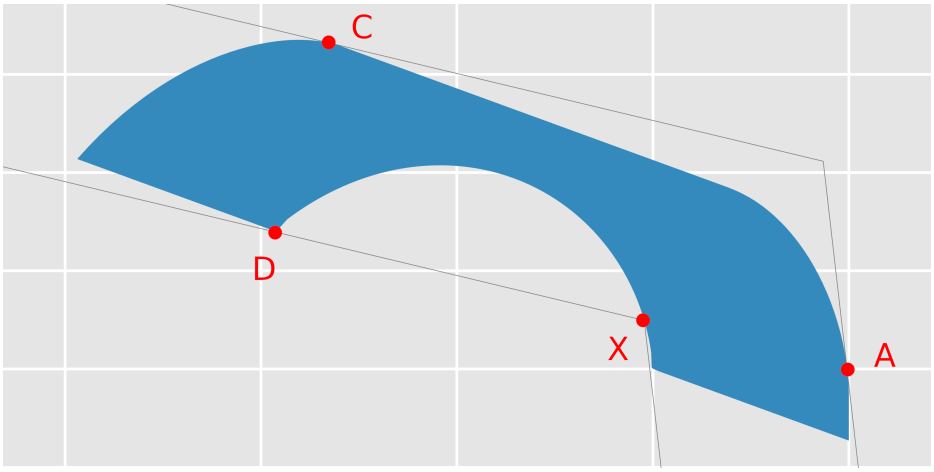

Figure 11: The First Tangency Case $x_2(t)$ for $\alpha = \pi/3$

Then, the case of $\{\mathbf{x}, \mathbf{A}, \mathbf{C}\}$ occurs.

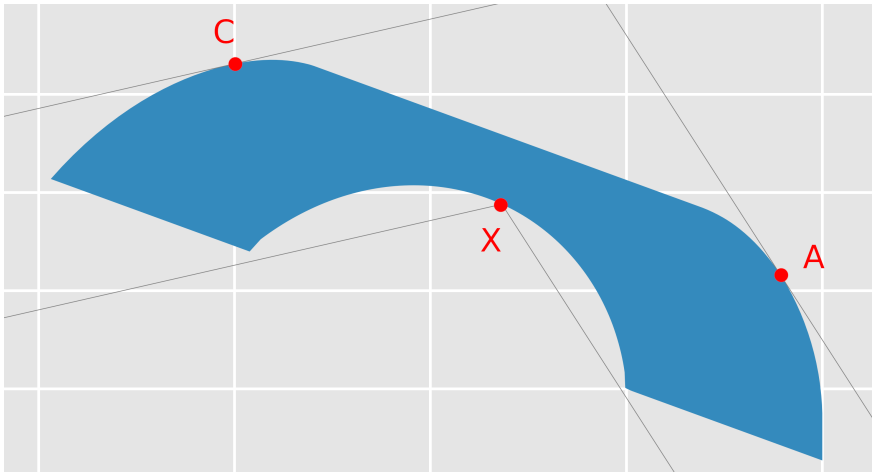

Figure 12: The Second Tangency Case $x_3(t)$ for $\alpha = \pi/3$

The final tangency case is symmetric to the first with the points $\{\mathbf{x}, \mathbf{A}, \mathbf{C}, \mathbf{B}\}$ which corresponds to $\mathbf{x}_4(t)$. The picture of this case is omitted.

Immediately, an issue in our plan of attack arises. One of the most important assumptions Romik made when solving for the unknown constants in his system was that the sofa shape would be symmetric. More specifically, he assumed that

$$x'(\pi/2 - t) = \begin{pmatrix} 1 & 0 \\ 0 & -1 \end{pmatrix} x'(t)$$

This reduced the number of equations needed to solve for all of the unknowns by half. Unfortunately, the middle case of $\{\mathbf{x}, \mathbf{A}, \mathbf{C}\}$ corresponding to $\mathbf{x}_3(t)$ is not symmetric over any open interval. This is additionally problematic because we need to introduce two new unknowns θ, ϕ which satisfy

$$x_2(\theta) = x_3(\theta) \quad \text{and} \quad x_3(\phi) = x_4(\phi)$$

This leaves no clear path for solving for the unknown constants introduced by $x_3(t)$. Surprisingly, we will soon see that this ends up not being an issue.

8.1 Four New Candidate Non-unique Maximums for $\alpha < \pi/2$

We will search for the rotation path satisfying the following assumptions:

1. The rotation path satisfies $\mathbf{x}(0) = \begin{pmatrix} 0 & 0 \end{pmatrix}^T$
2. The contact point $\mathbf{A}$ satisfies $\mathbf{A}(0) = \big(1, -\cot(\pi/3)\big)$
3. The rotation path is continuously differentiable.
4. The rotation path satisfies $\mathbf{x}(\pi/3) \cdot \mathbf{q}_0 = 0$.
5. The rotation path is well-behaved as defined in theorem 6.2.
6. The rotation path follows the piecewise definition

$$\mathbf{x}(t) = \begin{cases} \mathbf{x}_2(t) & t \leq \pi/6 \\ \mathbf{x}_4(t) & t > \pi/6 \end{cases}$$

Assumption 6 alone gives rise to a system of eight unknown constants $f_1, f_2, h_1, h_2, k_{21}, k_{22}, k_{41}$, and k_{42}. Assumptions 1 and 2 translate to three linear relations between the unknown constants. In particular,

$$f_2 = \frac{4(1+\pi)f_1}{\sqrt{3}(\pi-3)} + \frac{16(1+\pi)}{3(\pi-3)} \tag{23}$$

$$k_{21} = -\frac{\sqrt{3}(5+9\pi)f_1}{8(\pi-3)} - \frac{(7+3\pi)}{\pi-3} \tag{24}$$

$$k_{22} = \frac{(7+3\pi)}{\sqrt{3}(\pi-3)} - \frac{f_1(-11-7\pi)}{8(\pi-3)} \tag{25}$$

Assumption 4 is equivalent to saying that the rotation path begins on the bottom edge of L_{horiz} and returns to the same at possibly a different spot. Assumption 3 can be equivalently stated as

$$\mathbf{x}_2(\pi/6) = \mathbf{x}_4(\pi/6)$$

and at the same time

$$\mathbf{x'}_2(\pi/6) = \mathbf{x'}_4(\pi/6)$$

These two assumptions lead to new linear relations between unknown constants.

$$h_2 = -\frac{(17+5\pi)f_1}{4\sqrt{3}(5+\pi)} + \frac{e^{-\frac{\pi}{3\sqrt{3}}}(3\pi-1)h_1}{3(5+\pi)} - \frac{e^{-\frac{\pi}{6\sqrt{3}}}(9+5\pi)}{2(5+\pi)} \tag{26}$$

$$f_2 = -\frac{e^{\frac{\pi}{3\sqrt{3}}}(1+\pi)f_1}{\sqrt{3}(5+\pi)} + \frac{8(1+\pi)h_1}{3(5+\pi)} - \frac{4e^{\frac{\pi}{6\sqrt{3}}}(1+\pi)}{5+\pi} \tag{27}$$

$$k_{41} = -\frac{e^{\frac{\pi}{6\sqrt{3}}}(3\pi-1)f_1}{8(5+\pi)} + \frac{e^{-\frac{\pi}{6\sqrt{3}}}(3\pi-1)h_1}{\sqrt{3}(5+\pi)} + k_{21} - \frac{\sqrt{3}(3+7\pi)}{4(5+\pi)} \tag{28}$$

$$k_{42} = \frac{1}{8}\sqrt{3}e^{\frac{\pi}{6\sqrt{3}}}f_1 + k_{22} + \frac{1}{4} \tag{29}$$

Luckily both of our sets of linear relations give an expression for f_2. In the first set, f_2 is expressed in terms of f_1 and in the second f_2 is expressed in terms of f_1 and h_1 allowing us to unravel the system. Now, to find the numerical values of the unknown constants we are able to plug in the above expressions into Mathematica's *FindRoot* function. This function will return the numerical values to any desired level of precision The values of the constant terms are given below.

$f_1 = -2.2576050436918795...$	$k_{21} = -1.1353347513727689...$
$f_2 = 3.4988274416800403...$	$k_{22} = 1.2198870852483749...$
$h_1 = 3.7139822931046326...$	$k_{41} = -0.42941735366392529...$
$h_2 = 0.8873984405485661...$	$k_{42} = 0.8085760300694581...$

Table 1: Numerical Solutions of Constant Coefficients

Now we have a fully defined area-maximizing rotation path given the assumptions made at the beginning of this section. We plotted the piecewise boundary of the shape and delineated transitions between boundary definitions (for example, the transition from $\mathbf{x}_2(t) \to \mathbf{x}_4(t)$) with small ticks.

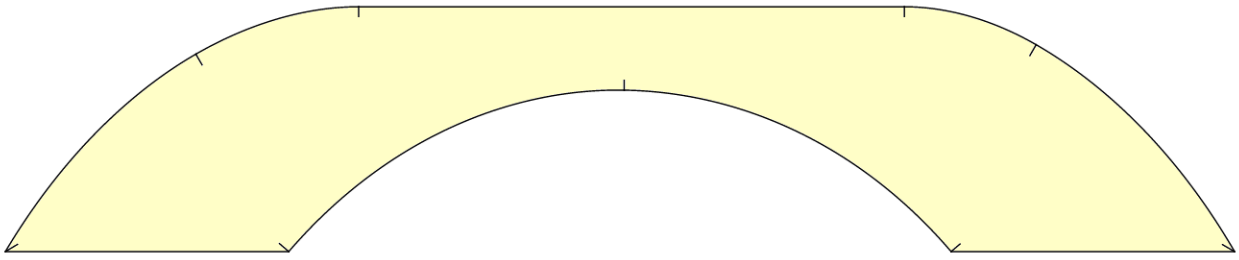

Figure 13: $\mathbf{S}$: A Conjectured Solution for the $\alpha = \pi/3$ Case

For ease of reference we will call this new sofa shape $\mathbb{S}$. Using Mathematica's numerical integration method *NIntegrate*, we integrate over the piecewise defined boundary lines of $\mathbb{S}$ to find its area of 2.895484047527441.... Naturally, the next step is to compare this area value to that of the discrete approximation produced by the algorithm. As it turns out, for $N = 64$ the area of the discrete approximation is 2.89580771204.... Since the algorithm

produces elements of a sequence which converge in area from above (a result given by Gerver) this is very good evidence that the area of $\mathbb{S}$ is close to if not the maximum area for the $\alpha = \pi/3$ case. One of the most striking features of $\mathbb{S}$ is the fact that it transitions through the tangency case of $\{\mathbf{x}, \mathbf{A}, \mathbf{C}\}$ corresponding to $\mathbf{x}_3(t)$ without actually containing $\mathbf{x}_3(t)$ as part of the rotation path definition (since we defined it to be just composed of $\mathbf{x}_2(t)$ and $\mathbf{x}_4(t)$). This is particularly odd, since the derivation of $\mathbf{x}_2(t)$ and $\mathbf{x}_4(t)$ makes the assumption that at least one of the contact points $\mathbf{B}$ or $\mathbf{D}$ is tangent to the sofa shape for any given t. However, the shape produced by these rotation paths produces a shape which seems to directly contradict that assumption. However, there is a surprisingly simple explanation for this. Before diving in, the figure in section 3 is a quick visual refresher on the definitions of the contact points if you are in need.

Let $\hat{x}_\pm, \hat{D}_\pm, \hat{C}_\pm$ be the absolute areas gained $(+)$ or lost $(-)$ around the respective contact points given a perturbation of $\mathbf{x}$ towards or away from $\mathbf{C}$ (equivalently along $\pm\mathbf{q}_t$). Since $\mathbf{x}_2(t)$ corresponds to the case of tangency $\{\mathbf{x}, \mathbf{A}, \mathbf{C}, \mathbf{D}\}$, when perturbations are made towards $\mathbf{C}$ along $\mathbf{q}_t$ for the rotation path to be area maximizing it must be that

$$\hat{C}_+ - (\hat{x}_- + \hat{D}_-) \leq 0 \quad \text{ and } (\hat{x}_+ + \hat{D}_+) - \hat{C}_- \leq 0$$

. Now consider a small range of t where the points of tangency are $\{\mathbf{x}, \mathbf{A}, \mathbf{C}\}$ corresponding to $\mathbf{x}_3(t)$. In this case For small enough perturbations towards and away from $\mathbf{C}$ along $\mathbf{q}_t$, it must be that

$$\hat{C}_+ - \hat{x}_- \leq 0 \quad \text{ and } \hat{x}_+ - \hat{C}_- \leq 0$$

Note that when the tangency case corresponding to $\mathbf{x}_3(t)$ occurs the area lost around the contact point $\mathbf{D}$ is *zero* since the contact point does not touch the boundary of the shape. Trivially, for pushes in the other direction the area gained is also zero. In other words, when $\hat{D}_\pm = 0$,

$$\hat{C}_+ - (\hat{x}_- + \hat{D}_-) = \hat{C}_+ - \hat{x}_- \leq 0$$

and

$$(\hat{x}_+ + \hat{D}_+) - \hat{C}_- = \hat{x}_+ - \hat{C}_- \leq 0$$

which shows that the area maximizing assumptions made about $\mathbf{x}_3(t)$ are satisfied by $\mathbf{x}_2(t)$.

This explains how we ended up with an unexpected tangency case corresponding to $\mathbf{x}_3(t)$ in our solution. There are still surprising features of $\mathbb{S}$ to discuss. Let $\mathbf{A}_i(t), \mathbf{C}_i(t)$ be the corresponding rotation point to $\mathbf{x}_i(t)$. Note the unequal distribution of tick marks on the top edge of $\mathbb{S}$. In fact, none of the five line segments making up the top edge of $\mathbb{S}$ are of equal length. However, the following relation holds

$$\frac{d}{dt}\mathbf{A}_2(\pi/6) = \frac{d}{dt}\mathbf{A}_4(\pi/6) = -\frac{d}{dt}\mathbf{C}_2(\pi/6) = -\frac{d}{dt}\mathbf{C}_4(\pi/6)$$

This implies that there is, in some sense, an 'optimal' slope at which the top boundary must transition at to be the optimal. This could possibly help reduce the number of assumptions needed to simplify the system of unknowns for future derivations of new αs. The asymmetric distribution of the ticks on the top edge also begs the question of whether $\mathbb{S}$ is symmetric or not.

Taking the plot of $\mathbb{S}$, we can copy and mirror it, and place it over the original plot with 50% opacity. In figure 14 we see that this reveals the asymmetry of $\mathbb{S}$ on each of its outward facing edges while the rotation path appears symmetric by visual inspection.

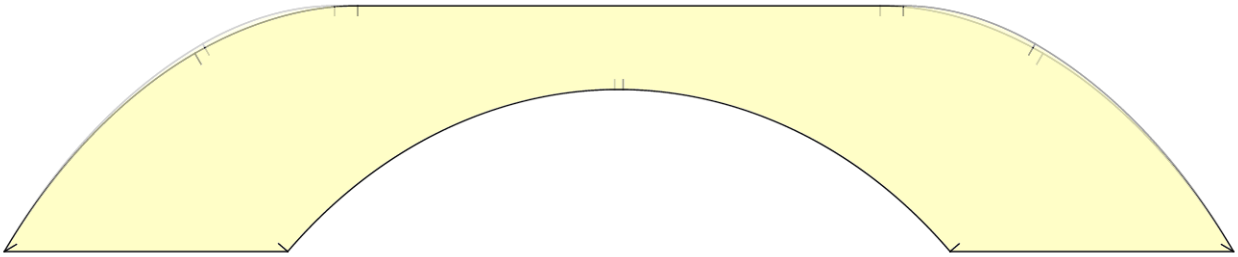

Figure 14: The asymmetry of $\mathbb{S}$

This is particularly exciting as shows that if $\mathbb{S}$ is the maximum for the $\alpha = \pi/3$ case, then the maximum is nonunique. This is because the hallway is symmetric across the line connecting the inner corner $(0, 0)$ and the outer corner which is at $(1, 1)$ for $\alpha = \pi/2$ but has a rather long expression for general values of α. Then, it's the case that reflections of the hallway across the line of symmetry are subsets of the non-reflected hallway which immediately gives that the reflection of an asymmetric maximum is also a maximum.

For $\alpha < 4\pi/9$, the discrete approximations outputted by the algorithm and the constructions derived from the differential equations agree to a high degree of accuracy in geometry and area. The algorithm and differential equation method agree in area for up to $\alpha = 17\pi/36$ but its not clear whether the geometry agrees or not so for now we omit those results. Using the same assumptions as we made at the beginning of the section, deriving new candidate solutions for the modified moving sofa problem for various α becomes procedural. Below are the plots for $\alpha = 7\pi/18$, $\alpha = 5\pi/18$, and $\alpha = 2\pi/9$ (not to scale).

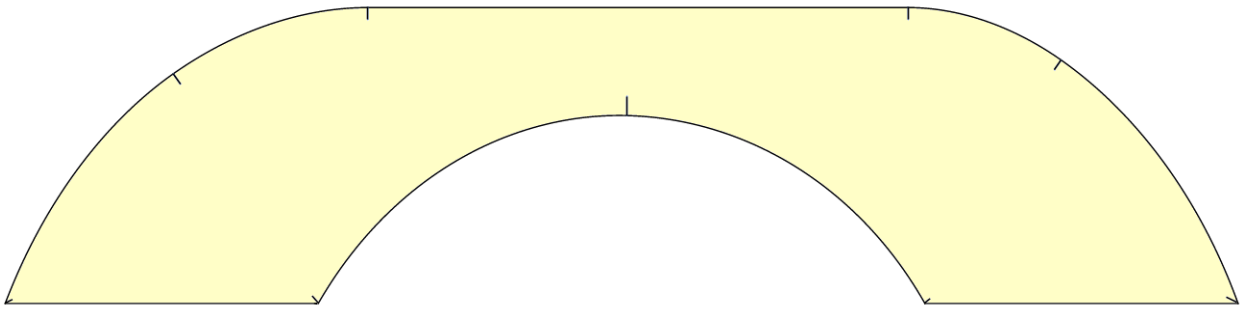

Figure 15: Candidate Solution for $\alpha = 7\pi/18$

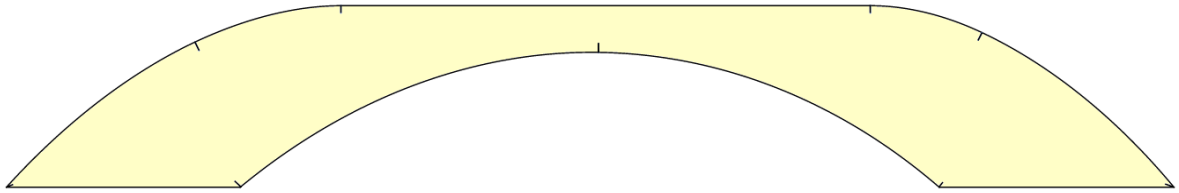

Figure 16: Candidate Solution for $\alpha = 5\pi/18$

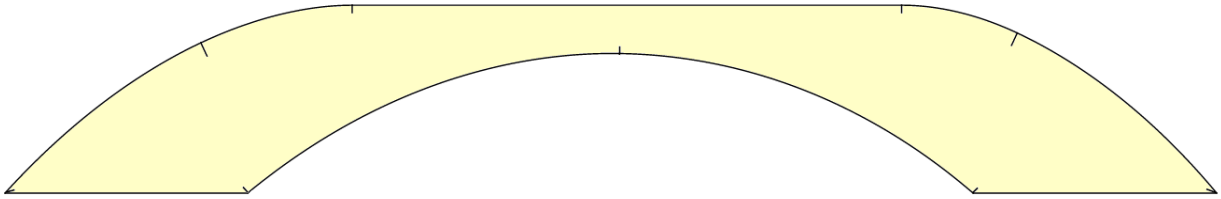

Figure 17: Candidate Solution for $\alpha = 2\pi/9$

We also derived a candidate solution for the $\alpha = \pi/180$ case out of curiosity. The candidate solution is over 300 units long so it cannot be reasonably displayed here. The following table gives the conjectured area of the solution to the moving sofa problem and the modified moving sofa problem.

degree bend	area
$\pi/2$	2.21958...
$7\pi/18$	2.58259...
$5\pi/18$	3.32961...
$2\pi/9$	3.94031...
$\pi/180$	154.068...

Table 2: Conjectured Maximum Solution Area

9 Going Forward

We've shown how solutions for other values of α can be be derived by extending Romik's results to non-$\alpha = \pi/2$ hallways. The results are exciting, but need to be made more rigorous before any conclusions can be drawn. Here are some remaining open problems:

1. Prove that Gerver's sofa is or is not the local or global maximum for the $\alpha = \pi/2$ case.

2. Prove that the shapes for non-$\pi/2$ alphas in this paper are local or global maximum. Show rigorously that the shapes given in this paper for the non-$\pi/2$ alphas are asymmetric. This is probably one of the conceptually simplest open problems. Is the order of the rotation path pieces correct for the $\alpha = 7\pi/18$ case? What about the other cases? Can we prove that some rotation path piece orders cannot produce the maximum?

3. Can we use the same method to construct sofas for $\alpha > 90$? The answer is almost certainly yes, but it will require the derivation of new tangency cases $\Gamma_{\mathbf{x}} = \{\mathbf{C}, \mathbf{D}\}$ and $\Gamma_{\mathbf{x}} = \{\mathbf{A}, \mathbf{B}\}$ for $t = 0$ and $t = \alpha$ respectively. The need for these cases was derived from the output of the algorithm. Do these shapes have asymmetry?

4. Can a method more rigorous than the algorithm be made to make reasonable assumptions to reduce the number of unknowns in the rotation path? It's possible that the algorithm converges to local, but not global, optimums.

References

1. D. Romik. Differential equations and exact solutions in the moving sofa problem. *Experimental Math* **27** (2018), 316-330.

2. J. Hammersley. On the Enfeeblement of Mathematical Skills by Modern Mathematics and by Similar Soft Intellectual Trash in Schools and Universities. *Bull. Inst. Math. App.* **4** (1968), 66-85.

3. J.L. Gerver. On moving a sofa around a corner. *Geometriae Dedicata* **42** (1992), 267-283.

4. W. Boyce, R. DePrima. Elementary Differential Equations and Boundary Value Problems.

5. Society of Applied and Industrial Mathematrics, and Murray Klamkin. "Problems and Solutions." *SIAM Review*, vol. 1, no. 1, 1967, pp.75-78.